



Optimization via Rejection-Free Partial Neighbor Search

Sigeng Chen¹ · Jeffrey S. Rosenthal¹ · Aki Dote² · Hirotaka Tamura³ · Ali Sheikholeslami⁴

Received: 30 September 2022 / Accepted: 19 September 2023

© The Author(s), under exclusive licence to Springer Science+Business Media, LLC, part of Springer Nature 2023

Abstract

Simulated Annealing using Metropolis steps at decreasing temperatures is widely used to solve complex combinatorial optimization problems (Kirkpatrick et al. in *Science* 220(4598):671–680, 1983). To improve its efficiency, we can use the Rejection-Free version of the Metropolis algorithm, which avoids the inefficiency of rejections by considering all the neighbors at every step (Rosenthal et al. in *Comput Stat* 36(4):2789–2811, 2021). To prevent the algorithm from becoming stuck in local extreme areas, we propose an enhanced version of Rejection-Free called Partial Neighbor Search, which only considers random parts of the neighbors while applying Rejection-Free. We demonstrate the superior performance of the Rejection-Free Partial Neighbor Search algorithm compared to the Simulation Annealing and Rejection-Free with several examples, such as the QUBO question, the Knapsack problem, the 3R3XOR problem, and the quadratic programming.

Keywords Simulated Annealing · Rejection-Free · Partial Neighbor Search · QUBO

1 Introduction

Optimization is the cornerstone of many areas. It plays a crucial role in finding feasible solutions to real-life problems, from mathematical programming to operations research, economics, management science, business, medicine, life science, and artificial intelligence (Floudas and Pardalos 2008). Before the invention of linear and integer program-

ming in the 1950s, optimization was characterized by several independent topics, such as optimum assignment, the shortest spanning tree, transportation, and the traveling salesman problem, which were then united into one framework (Schrijver 2005). Today, combinatorial optimization is essential in research because most problems originate from practice and are dealt with daily (Schrijver 2005). Optimization questions aim to find an optimal solution to maximize or minimize a real function within a given state space. Sometimes, a feasible solution with the corresponding function value near the optimal solution is also acceptable. The process of finding an optimal or feasible solution to some complex combinatorial optimization problems may take a considerable amount of time. In particular, no algorithm for NP-hard problems can guarantee that the optimal state of the problem will be found within a limitation governed by a polynomial based on the input length (Garey et al. 1974).

Among all complex optimization problem solvers, meta-heuristics are usually nature-inspired (Bianchi et al. 2009). They are designed to select a heuristic that often arrives at a feasible solution instead of an optimal one. The Simulated Annealing algorithm (Kirkpatrick et al. 1983), based on the Metropolis steps (Metropolis et al. 1953) at decreasing temperatures, is a typical method of this kind. The Simulated Annealing algorithm, however, may be inefficient because of frequent rejections. To improve the performance of Simulated Annealing, we adopt the Rejection-Free algorithm for

✉ Sigeng Chen
sigeng.chen@mail.utoronto.ca

Jeffrey S. Rosenthal
jeff@math.toronto.edu

Aki Dote
dote.aki@fujitsu.com

Hirotaka Tamura
tamura.hirotaka@dxrllab.com

Ali Sheikholeslami
ali@ece.utoronto.ca

¹ Department of Statistical Sciences, University of Toronto, 700 University Avenue, Toronto, ON M5G 1Z5, Canada

² Fujitsu Ltd., 4-1-1 Kamikodanaka, Nakahara-ku, Kawasaki, Kanagawa 211-8588, Japan

³ DXR Laboratory Inc., 4-38-10 Takata-Nishi, Kohoku-ku, Yokohama, Kanagawa 223-0066, Japan

⁴ Department of Electrical and Computer Engineering, University of Toronto, 10 King's College Road, Toronto, ON M5S 3G4, Canada

sampling (Rosenthal et al. 2021; Douc and Robert 2011) into an optimization version. Additionally, Rejection-Free may experience inefficiency when it enters local extreme areas. Therefore, we propose another algorithm based on the Rejection-Free algorithm called Partial Neighbor Search (PNS) to enhance its efficiency further.

Rejection-Free and PNS are more efficient in many optimization problems than Simulated Annealing, even when applied to a single-core implementation. The implementation of these algorithms can also be carried out through parallelism to increase efficiency even further. It is possible to use processors designed for general purposes, such as Intel and AMD cores, for parallel computing to accelerate the algorithm to some extent. However, these chips were not built for parallel computing, and off-chip communication significantly slows the data transfer rate to and from the cores (Sodan et al. 2010). On the other hand, parallelism hardware explicitly designed for MCMC trials has been created. For example, the second generation of Fujitsu Digital Annealer uses a dedicated processor called Digital Annealing Unit (DAU) (Matsubara et al. 2020) to achieve high speed. This dedicated processor is designed to minimize communication overhead in arithmetic circuitry and with memory. It can achieve 100x to 10,000x speedups by combining Rejection-Free and PNS with such parallelism hardware (Sheikholeslami 2021).

This paper aims to propose a new metaheuristic algorithm called Partial Neighbor Search to find a feasible solution in optimization questions efficiently. We next review the Simulated Annealing algorithm, the Metropolis algorithm, and the Rejection-Free algorithm for sampling. Following that, Sect. 2 describes how to use the Rejection-Free algorithm to solve optimization problems. Our next point is that the local maximum may lead to another kind of inefficiency for Rejection-Free, and Sect. 3 introduces our Partial Neighbor Search (PNS) algorithm for optimization, which considers just subsets of neighbor states for possible moves. In Sect. 4, we demonstrate how PNS can be applied to quadratic unconstrained binary optimization (QUBO) questions and its effectiveness in solving them. We then discuss why this improvement occurs (Sect. 5), and how its subsets of partial neighbors should be chosen (Sect. 6), as well as its relation to the Tabu Search algorithm (Sect. 7). Moreover, we present several other examples, such as the Knapsack problem (Sect. 8) and the 3R3XOR problem (Sect. 9), to illustrate the advantages of the PNS algorithm in discrete optimization problems. Furthermore, Sect. 10 demonstrates another advantage of PNS over Rejection-Free by providing a continuous optimization example known as quadratic programming. PNS can easily be adapted to the general state space by selecting only a finite subset, and it outperforms Simulated Annealing. In contrast, Rejection-Free cannot be

applied in this case due to the need to consider all neighbors at each step.

1.1 Background on Simulated Annealing for optimization

Simulated Annealing, as introduced by Kirkpatrick et al. (1983), is widely used to solve combinatorial optimization problems, such as approximating the optimal values of functions with many variables (Rutenbar 1989). Although there is some theory to prove that Simulated Annealing will converge to the optimal solution almost surely with sufficiently slow cooling schedules (Nikolaev and Jacobson 2010), for many complex optimization problems, such as NP-hard problems, there is no guarantee that this algorithm will provide an optimal solution within a reasonable amount of time. On the other hand, Simulated Annealing can give reasonable, feasible solutions quickly (Albright 2007). Discrete Simulated Annealing contains the following essential elements (Bertsimas and Tsitsiklis 1993):

1. A state space \mathcal{S} .
2. A real-valued target density π on \mathcal{S} . The ultimate goal for the Simulated Annealing is to find $y \in \mathcal{S}$ such that $\pi(y) > \pi(x), \forall x \in \mathcal{S}$. However, for many circumstances, a good feasible solution is acceptable.
3. $\forall x \in \mathcal{S}, \exists$ a proposal distribution $Q(x, \cdot)$ where $\sum_{y \in \mathcal{S} \setminus \{x\}} Q(x, y) = 1$.
4. $\forall x \in \mathcal{S}, \exists \mathcal{N}(x) = \{y \in \mathcal{S} \mid Q(x, y) > 0\} \subset \mathcal{S} \setminus \{x\}$, called the neighbors of x .
5. A non-increasing function $T : \mathbb{N} \rightarrow (0, \infty)$, called the Cooling Schedule. $T(k)$ is called the temperature at step $k \in \mathbb{N}$.
6. An initial State $X_0 \in \mathcal{S}$.

We discuss the discrete cases here first, and then in Sect. 10, we will talk more about optimization in general state space. With the above elements, the Simulated Annealing algorithm, which consists of a discrete time-inhomogeneous Markov Chain $\{X_k\}_{k=0}^K$ can be generated by Algorithm 1. Algorithm 1 is designed to find X_k such that $\pi(X_k) \approx \sup_{x \in \mathcal{S}} \pi(x)$ with high probability, though that is not guaranteed. Note that the algorithm can also be formulated using log values for better numerical stability.

1.2 Background on Metropolis-Hastings algorithm

The above Simulated Annealing algorithm is designed based on the Metropolis algorithm (Metropolis et al. 1953). Among all the Monte Carlo algorithms, the Metropolis algorithm has been the most successful and influential (Beichl and Sullivan 2000). It is designed to generate a Markov chain that converges to a given target density π on a state space

Algorithm 1 Simulated Annealing

```

initialize  $X_0$ 
for  $k$  in 1 to  $K$  do
  random  $Y \in \mathcal{N}(X_{k-1})$  based on  $\mathcal{Q}(X_{k-1}, \cdot)$ 
  random  $U_k \sim \text{Uniform}(0, 1)$ 
  if  $U_k < [\frac{\pi(Y)}{\pi(X_{k-1})}]^{1/T(k)}$  then
     $\triangleright$  accept with probability  $\min \left\{ 1, [\frac{\pi(Y)}{\pi(X_{k-1})}]^{1/T(k)} \right\}$ 
     $X_k = Y$   $\triangleright$  accept and move to state  $Y$ 
  else
     $X_k = X_{k-1}$   $\triangleright$  reject and stay at  $X_{k-1}$ 
  end if
end for
    
```

\mathcal{S} . As a generalization of the Metropolis algorithm, the Metropolis-Hastings algorithm includes the possibility of a non-symmetric proposal distribution \mathcal{Q} (Hitchcock 2003). The Metropolis-Hastings algorithm is described in Algorithm 2.

Algorithm 2 the Metropolis-Hastings algorithm

```

initialize  $X_0$ 
for  $k$  in 1 to  $K$  do
  random  $Y \in \mathcal{N}(X_{k-1})$  based on  $\mathcal{Q}(X_{k-1}, \cdot)$ 
  random  $U_k \sim \text{Uniform}(0, 1)$ 
  if  $U_k < \frac{\pi(Y)\mathcal{Q}(Y, X_{k-1})}{\pi(X_{k-1})\mathcal{Q}(X_{k-1}, Y)}$  then
     $\triangleright$  accept with probability  $\min \left\{ 1, \frac{\pi(Y)\mathcal{Q}(Y, X_{k-1})}{\pi(X_{k-1})\mathcal{Q}(X_{k-1}, Y)} \right\}$ 
     $X_k \leftarrow Y$   $\triangleright$  accept and move to state  $Y$ 
  else
     $X_k \leftarrow X_{k-1}$   $\triangleright$  reject and stay at  $X_{k-1}$ 
  end if
end for
    
```

Algorithm 2 ensures the Markov chain $\{X_0, X_1, X_2, \dots, X_K\}$ has π as stationary distribution. It follows (assuming irreducibility) that the expected value $E_\pi(h)$ of a functional $h : \mathcal{S} \rightarrow \mathbb{R}$ with respect to π can be estimated by $\frac{1}{M} \sum_{i=1}^M h(X_i)$ for sufficiently large run length M . Although the Metropolis-Hastings algorithm and Simulated Annealing are designed for different purposes, regarding the implementation, the Cooling Schedule is the only difference between them. Thus, both Simulated Annealing and the Metropolis-Hastings algorithm may face inefficiencies from the rejections (Rosenthal et al. 2021).

1.3 Background on Rejection-Free algorithm for sampling

Rejections in both Simulated Annealing and the Metropolis-Hastings algorithm may slow down the efficiency of the algorithm. In Algorithm 1, if $U_k \geq [\frac{\pi(Y)}{\pi(X_k)}]^{1/T(k)}$, then we will remain at the current state, even though we have spent time in proposing a state, computing a ratio of target densities, generating a random variable U_k , and deciding not to accept the proposal. Such inefficiencies could happen frequently and

are considered a necessary evil of Simulated Annealing and the Metropolis-Hastings algorithm. However, we can compute all potential acceptance probabilities simultaneously to allow for the possibility of skipping these rejection steps. By removing the inefficiencies of rejections in both algorithms, the Rejection-Free algorithm can lead to significant speedup (Rosenthal et al. 2021; Douc and Robert 2011).

Before introducing Rejection-Free, we need to introduce the jump chain first. Given a run $\{X_k\}$ of a Markov chain, we define the jump chain to be $\{J_k, M_k\}$, where $\{J_k\}$ represents the same chain as $\{X_k\}$ except omitting any immediately repeated states, and the Multiplicity List $\{M_k\}$ is used to count the number of times the original chain remains at the same state.

For example, if the original chain is

$$\{X_k\} = \{a, b, b, b, a, a, c, c, c, c, d, d, a, \dots\}, \tag{1}$$

then the jump chain would be

$$\{J_k\} = \{a, b, a, c, d, a, \dots\}, \tag{2}$$

with the corresponding multiplicity list being

$$\{M_k\} = \{1, 3, 2, 4, 2, 1, \dots\}. \tag{3}$$

the jump chain $\{J_k, M_k\}$ itself is a Markov chain. If we use notation $P(y | x)$ to represent the transition probability from x to y by Metropolis-Hastings, the transition probabilities $\hat{P}(y | x)$ for the jump chain is specified by

$$\begin{aligned} \hat{P}(x | x) &:= 0 \\ \forall y \neq x, \hat{P}(y | x) &:= P[J_{k+1} = y | J_k = x] \\ &= \frac{P(y | x)}{\sum_{z \neq x} P(z | x)} \end{aligned} \tag{4}$$

Moreover, the conditional distribution of $\{M_k\}$ given $\{J_k\}$ is equal to the distribution of $1 + G$ where G is a geometric random variable with success probability $p = 1 - P(x | x) = \sum_{z \neq x} P(z | x)$; see Rosenthal et al. (2021), Douc and Robert (2011).

Given the above properties for the Jump chain, the Rejection-Free algorithm can be used for sampling as described by Algorithm 3. Algorithm 3 only works for the discrete cases where all states have at most finite neighbors. Theorem 13 in Rosenthal et al. (2021) extended the Rejection-Free to general state space, and we will discuss more by a continuous optimization question in Sect. 10.

Algorithm 3 ensures (assuming irreducibility) that the expected value $E_\pi(h)$ of a functional $h : \mathcal{S} \rightarrow \mathbb{R}$ with respect to π can be estimated by $\frac{\sum_{k=1}^K M_k h(J_k)}{\sum_{k=1}^K M_k}$ for sufficiently large run length K , while avoiding any rejections. Rejection-Free

Algorithm 3 Rejection-Free for Sampling (Discrete Cases)

```

initialize  $J_0$ 
for  $k$  in 1 to  $K$  do
   $p \leftarrow 0$   $\triangleright$   $p$  is used to record the success probability for  $M_{k-1}$ 
  for  $Y$  in  $\mathcal{N}(J_{k-1})$  do  $\triangleright$  only works for finite neighbors
    calculate  $q(Y) = \mathcal{Q}(Y, J_{k-1}) \min\{1, \frac{\pi(Y)}{\pi(J_{k-1})}\}$ 
     $\triangleright$  the transition prob. from  $J_{k-1}$  to  $Y$ 
     $p \leftarrow p + q(Y)$   $\triangleright p = \sum_{z \neq x} P(z | x)$ 
  end for
  choose  $J_k \in \mathcal{N}(J_{k-1})$  such that  $\hat{P}(J_k = Y | J_{k-1}) \propto q(Y)$ 
   $\triangleright$  choose the next jump chain state
  calculate  $M_{k-1} = 1 + G$  where  $G \sim \text{Geom}(p)$ 
   $\triangleright$  multiplicity list for current state
end for
    
```

can lead to great speedup in examples where the Metropolis algorithm frequently rejects (Rosenthal et al. 2021).

2 Rejection-Free algorithm for optimization

In addition to sampling, the above Rejection-Free algorithm can also be applied to optimization problems. Given a set \mathcal{S} and a real-valued target density π on the set \mathcal{S} , we can use the Rejection-Free algorithm to find $x \in \mathcal{S}$ that maximizes $\pi(x)$ by Algorithm 4. Algorithm 4 is also designed to find X_k such that $\pi(X_k) \approx \sup_{x \in \mathcal{S}} \pi(x)$ with high probability, and the efficiency is greatly improved by avoiding rejections. Although the purpose of sampling and optimization are different, regarding the implementation, Rejection-Free optimization is only different from Rejection-Free sampling by getting rid of the multiplicity list $\{M_k\}$.

Algorithm 4 Rejection-Free for Optimization (Discrete Cases)

```

initialize  $J_0$ 
for  $k$  in 1 to  $K$  do
  for  $Y \in \mathcal{N}(J_{k-1})$  do  $\triangleright$  only works for finite neighbors
    calculate  $q(Y) = \mathcal{Q}(Y, J_{k-1}) \min\{1, [\frac{\pi(Y)}{\pi(J_k)}]^{1/\tau(k)}\}$ 
     $\triangleright$  the transition prob. from  $J_{k-1}$  to  $Y$ 
  end for
  choose  $J_k \in \mathcal{N}(J_{k-1})$  such that  $\hat{P}(J_k = Y | J_{k-1}) \propto q(Y)$ 
   $\triangleright$  choose the next jump chain State
end for
    
```

Although the Rejection-Free algorithm for optimization can help reduce the inefficiency of rejections, local maximum areas of π can still be a problem. For example, we want to find $x \in \mathcal{S}$, which maximizes $\pi(x)$ from a state space starting at state A in Fig. 1. Here, we use a uniform proposal distribution \mathcal{Q} on the neighbor sets \mathcal{N} as shown in Fig. 1.

Note that, $\pi(A_1) = \pi(A_2) = \dots = \pi(A_n) = 0.01$ while $\pi(A) = \pi(B) = 100$. Then the probability of escaping from state A by one Metropolis step is $\frac{1}{n+1} + \frac{n}{n+1} \times \frac{1}{10000}$, where

$\frac{1}{n+1}$ represents the probability of moving from state A to state B , and $\frac{n}{n+1} \times \frac{1}{10000}$ is the probability of moving from state A to A_1, A_2, \dots, A_n . Thus, we will have many rejections using Simulated Annealing with constant temperature $T \equiv 1$. Cooling Schedules can help reduce the probability of rejection at the beginning of Simulated Annealing since T should be large during that time. However, as we move on in Simulated Annealing, we will be more and more likely to be trapped by local maximum areas like this.

The Rejection-Free algorithm for optimization can produce some speedup in this case, but the Rejection-Free chain will still be stuck by the local maximum area $\{\pi(A), \pi(B)\}$. If n , the number of other neighbors for A and B , is small, this chain will be switching between A and B for a long time, since

$$\begin{aligned} \hat{P}(J_1 = B | J_0 = A) &= \frac{\min\{1, \frac{\pi(B)}{\pi(A)}\}}{\sum_{z \neq A} \min\{1, \frac{\pi(z)}{\pi(A)}\}} \\ &= \frac{1}{1 + 0.0001 \times n} \approx 1 \\ \hat{P}(J_1 = A | J_0 = B) &\approx 1. \end{aligned} \tag{5}$$

To help our Markov chain escape from those local maximums in optimization, we propose another method called Partial Neighbor Search based on the Rejection-Free algorithm.

3 Proposed Search Algorithm: Partial Neighbor Search

Partial Neighbor Search (PNS) is an algorithm based on the Rejection-Free, also designed as a Markov chain used for optimization as described in Algorithm 5. Algorithm 5 is also intended to find X_k such that $\pi(X_k) \approx \sup_{x \in \mathcal{S}} \pi(x)$ with high probability, and the efficiency is improved even further by avoiding both rejections and traps in local maximum areas.

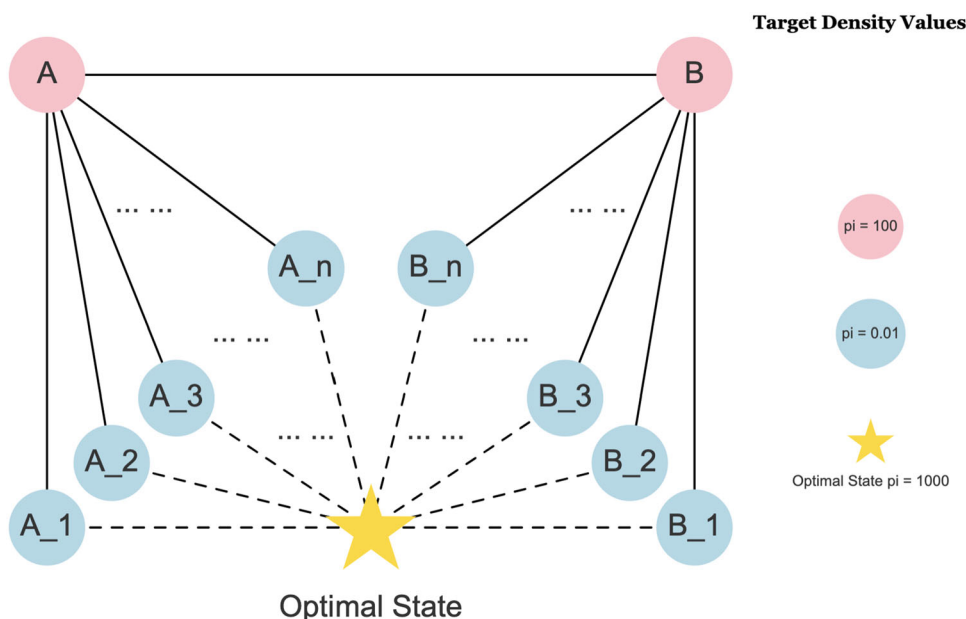
Algorithm 5 Partial Neighbor Search

```

initialize  $J_0$ 
for  $k$  in 1 to  $K$  do
  pick  $\mathcal{N}_k(J_{k-1}) \subset \mathcal{N}(J_{k-1})$  (★)
  for  $Y \in \mathcal{N}_k(J_{k-1})$  do  $\triangleright$  Only neighbors in  $\mathcal{N}_k$  will be considered
    calculate  $q(Y) = \mathcal{Q}(Y, J_{k-1}) \min\{1, [\frac{\pi(Y)}{\pi(J_k)}]^{1/\tau(k)}\}$ 
     $\triangleright$  the transition prob. from  $J_{k-1}$  to  $Y$ 
  end for
  choose  $J_k \in \mathcal{N}_k(J_{k-1})$  such that  $\hat{P}(J_k = Y | J_{k-1}) \propto q(Y)$ 
   $\triangleright$  choose the next Jump Chain State
end for
    
```

The (★) step in Algorithm 5 is the key of PNS. At this step, $\mathcal{N}_k(J_{k-1})$ could be random 50% of the elements from

Fig. 1 Illustration of the local maximum area in an optimization problem where both Simulated Annealing and Rejection-Free may get stuck. The target density π has the following function values:
 $\pi(A) = \pi(B) = 100$,
 $\pi(A_1) = \pi(A_2) = \dots = \pi(A_n) = \pi(B_1) = \pi(B_2) = \dots = \pi(B_n) = 0.01$



$\mathcal{N}(J_{k-1})$. In Sect. 6, we will explore many other choices for the (\star) step to figure out the best strategy. Moreover, for continuous cases, PNS can be applied, and we only need to ensure the Partial Neighbor Sets \mathcal{N}_k are always finite, $\forall k$. On the other hand, Algorithms 3 and Algorithm 4 for Rejection-Free only work for discrete cases where the number of neighbors for all states must be finite, and we will illustrate these by an optimization example in continuous cases in Sect. 10.

The motivation for PNS is simple: we have a better chance of escaping from the local maximum area if we force the algorithm to avoid some neighbors randomly. For example, in Fig. 1, if we only consider half of the neighbors at state A, we may disregard state B with probability 50%. That is, we have a probability of at least 50% of selecting a state from $\{A_1, A_2, \dots, A_n\}$ as our next state in the PNS chain. If this occurs, we are more likely to escape from the local maximum area $\{\pi(A), \pi(B)\}$.

4 Application to the QUBO question

The quadratic unconstrained binary optimization (QUBO) has gained increasing attention in combinatorial optimization due to its wide range of applications in finance and economics to machine learning (Kochenberger et al. 2014). The QUBO problem is known to be NP-hard (Glover et al. 2018), so it is common to use Simulated Annealing to find the optimal or workable solution. This problem can now be addressed using our PNS algorithm. (Additional applications are in Sects. 8, Sect. 9, and Sect. 10 below.)

For a given N by N matrix Q (usually upper triangular), the QUBO question aims to find

$$\arg \max x^T Qx, \text{ where } x \in \{0, 1\}^N \tag{6}$$

Sometimes $\arg \min$ is used instead of $\arg \max$, which is equivalent to taking the negative of Q , so for simplicity, we focus on the $\arg \max$ version here. In the simulation here, we use $N = 200$.

As part of our algorithm, we use a uniform proposal distribution among all neighbors where the neighbors are defined as binary vectors with Hamming distance 1. That is, $Q(x, y) = \frac{1}{N}$ for $\forall y \in \mathcal{N}(x)$, where $y \in \mathcal{N}(x) \iff |x - y| = \sum_{i=1}^N |x_i - y_i| = 1, \forall x, y \in \{0, 1\}^N$. We randomly choose half of the neighbors at each step of PNS, which means we only consider a random subset $\mathcal{N}_K(x) \subset \mathcal{N}(x)$ whose cardinality is $|\mathcal{N}_K(x)| = \frac{1}{2}|\mathcal{N}(x)| = \frac{1}{2}N$ for $\forall x \in \{0, 1\}^N$. In addition, the target density $\pi(x) = \exp\{x^T Qx\}$, since we need the target density to be positive all time to use the Cooling Schedule, and maximizing $x^T Qx$ is the same as maximizing $\exp\{x^T Qx\}$. Furthermore, $T(k)$ represents the temperature at step k for the cooling schedule.

We compare Simulated Annealing, Rejection-Free for Optimization, and PNS in 1000 simulation runs. We randomly generate a 200 by 200 upper triangular as the QUBO matrix Q . The non-zero elements from Q were generated randomly by $Q_{i,j} \sim \text{Normal}(0, 100^2), \forall i \leq j$.

The result for the simulation is shown in Fig. 2. Here, we used a violin plot to summarize the results. The violin plot uses the information available from local density estimates and the basic summary statistics to provide a valuable tool for data analysis and exploration (Hintze and Nelson 1998).

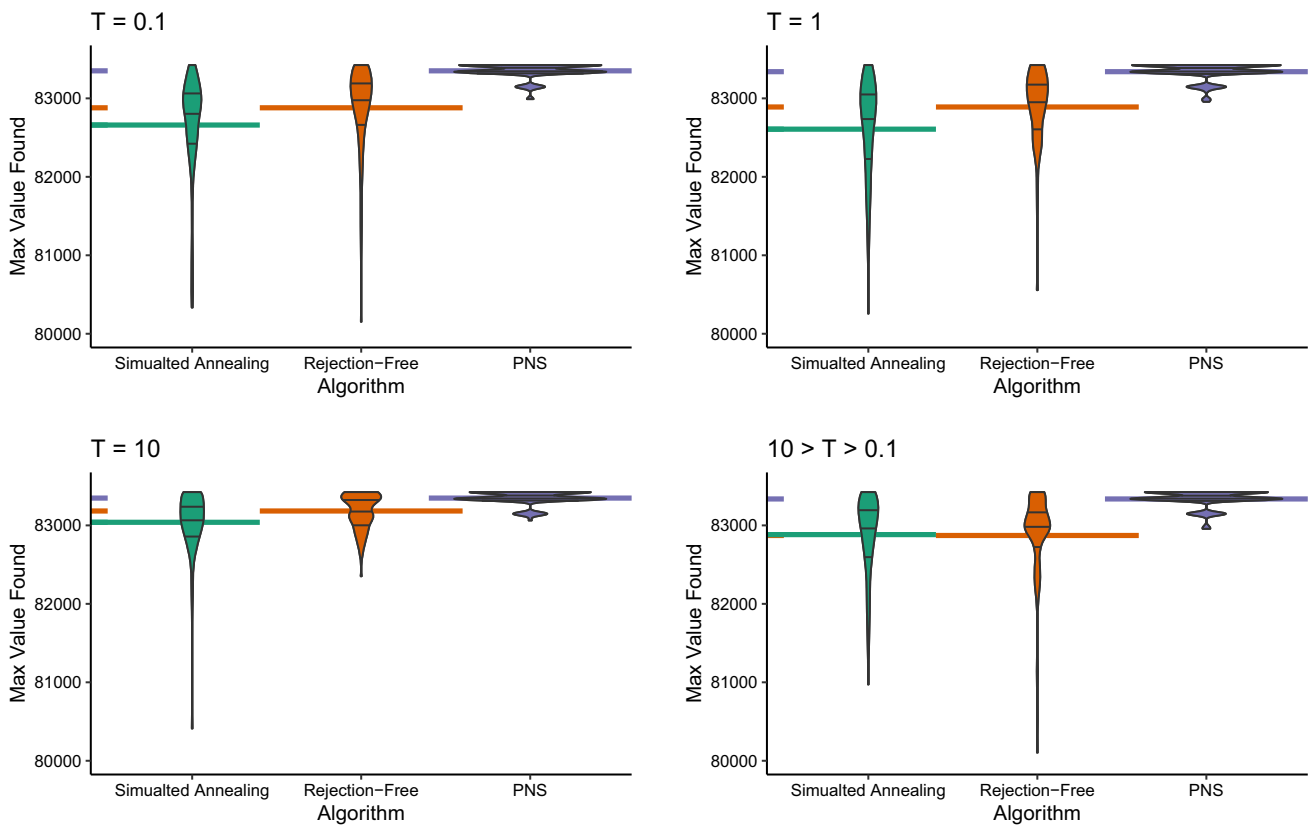


Fig. 2 Comparison of Simulated Annealing, Rejection-Free, and PNS in terms of the highest (log) target density value $\log \pi(x) = x^T Qx$ being found, for a random upper triangular QUBO matrix Q where the non-zero elements are generated by $Q_{i,j} \sim N(0, 100^2)$. Four different cooling schedules where $T(k) = 0.1, 1, \text{ and } 10$ constantly, and $T(k)$

being geometric from 10 to 0.1 are used here. The number of iterations for Simulated Annealing is 200,000, and the numbers of iterations for Rejection-Free and PNS are 1000. The three black lines inside the violin plots are 25%, 50%, and 75% quantile lines. The colored segments represent the mean values

To reveal the data structure, the violin plot combines two density traces on both sides and three quantile lines (25%, 50%, and 75%). In addition, we added a long segment of the bottom layer as the mean for the values. We also added a short segment on the y-axis to help compare the mean values.

Figure 2 shows that the PNS is always the best in all four different cooling schedules. Note that the number of iterations used for Simulated Annealing is 200,000 for Simulated Annealing while they are 1000 for both Rejection-Free and PNS. We used these many iterations because we need to consider 200 neighbors at each iteration in Rejection-Free. In contrast, we only need to consider one neighbor for each iteration in Simulated Annealing. If we proceed with all three algorithms on a single-core machine, the run time of a single simulation run for simulated Annealing is about 20 s; the run time for Rejection-Free is about 10 s; the run time for PNS is only 5 s. In addition, parallelism in computer hardware can increase the speed of both Rejection-Free and PNS by distributing the calculation of the transition probabilities for different neighbors onto different cores (Rosenthal et al. 2021). Besides that, we can also use multiple repli-

cas at different temperatures, such as in parallel tempering, or deploy a population of replicas at the same temperature (Sheikholeslami 2021). Combining these methods with parallelism hardware can yield 100x to 10,000x speedups for Rejection-Free and PNS (Sheikholeslami 2021).

In the above example, the improvement in the efficiency of Rejection-Free is easy to understand, while the performance of PNS is counter-intuitive. Compared to Rejection-Free, why would we get a better result by considering fewer neighbors at each step? To illustrate how PNS works, we can look closely at the Markov chains generated in the above example.

5 Understanding the improvement of Partial Neighbor Search

In this section, we found a local maximum area for the target density π purposefully in the previous QUBO example in Sect. 4 by looking at the final results from the simulation runs from the previous section. Many Rejection-Free chains stopped at this local maximum area after 1000 iterations. For

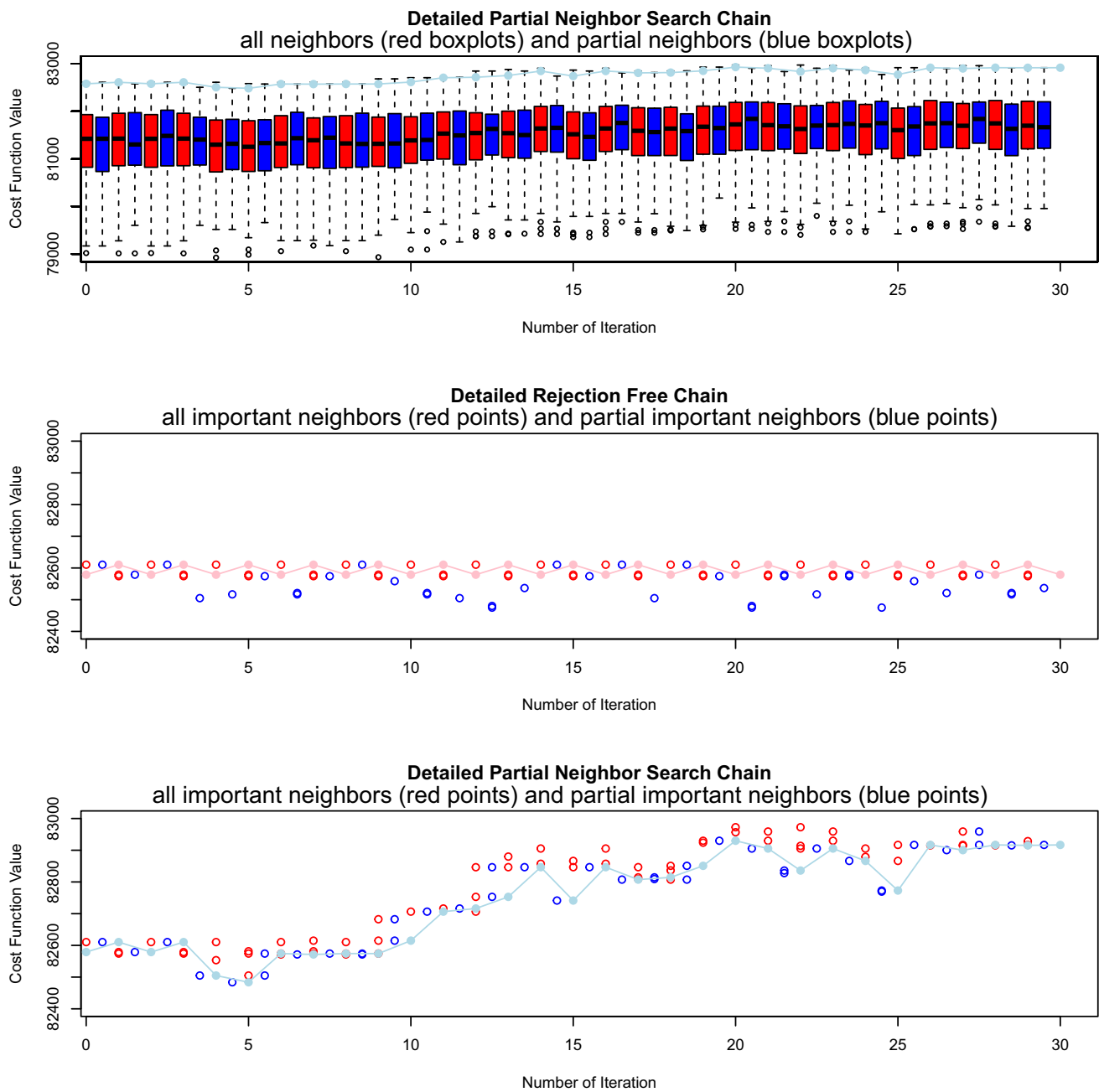


Fig. 3 The detailed Markov Chains from Rejection-Free (the pink chain in the second plot) and PNS (the light blue chain in the first and the third plot). The red box plots in the first plot represent the target density values for all neighbors, and the blue box plots represent the partial neighbors. Most of these values are useless because they are too small to be picked by the Markov chain. The second and the third plots only show the important neighbors, defined as those whose transition probability is

larger than $\exp\{-10\}$ times the highest transition probability among all neighbors. Here, red points represent all important neighbors, and blue points mean important neighbors of a random subset of all neighbors used for PNS. The Rejection-Free Chain switches between three local maximum states all the time while the PNS chain escapes from the local maximum area after five iterations. (Color figure online)

this local maximum area, the target density value is around 82600. This area contains three states whose target density values are much larger than all their other neighbors. Thus, this local maximum can trap the regular Rejection-Free chain for a long time, just like the cases we mentioned in Fig. 1. We can plot the Markov chains by PNS with the target density

values for all the neighbors by Rejection-Free and the random subset of neighbors by PNS in the form of boxplots. The boxplot of the first 30 steps from the first simulation in PNS is shown in the first plot in Fig. 3

From the first plot in Fig. 3, most of the target density values within the boxplot are not useful since they are too small

to be picked by the algorithm. Therefore, we only need to consider the important neighbors likely to be chosen. Firstly, for each state J_k in the Markov Chain, we find the max value among all the transition probabilities, and we define the important neighbors to be those neighbors whose transition probability is larger than $\exp\{-10\}$ times the highest transition probability among all neighbors. That is, for each J_k from the chain, we find $q(Y_0) = \max\{q(Y) \mid Y \in \mathcal{N}(J_k)\}$, and then we define $\{Y \mid Y \in \mathcal{N}(J_k), q(Y) > \exp\{-10\} \times q(Y_0)\}$ to be important neighbors for J_k . This time, we only have several important neighbors at each step. Thus, we used points instead of boxplots to show the important neighbors. The result from Rejection-Free and PNS is also shown in Fig. 3.

From the second plot in Fig. 3, the red dots represent the important neighbors, and the pink line means the Rejection-Free chain. We can see that this local maximum area of three states can easily trap the Rejection-Free chains because their target density values are much higher than all other neighbors. Thus, the important neighbors for any of these three states are only the remaining two, and the Rejection-Free chain will be switching between these three for a long time. At the same time, the blue dots in the second plot represent the important neighbors if we start to do PNS from that state. Although we did not apply PNS in the second plot, we still put the random subset for PNS there as a comparison. From the blue dots in the second plot, we can say that if we perform PNS, then the Markov chain can escape from this local maximum area faster since some groups of the blue dots do not contain any of these three states with high target density values.

On the other hand, the third plot in Fig. 3 shows that the PNS chain (blue line) escapes from this local maximum area within five steps. Again, the blue dots represent the important neighbor from PNS, and the red dots represent the important neighbor if we start to perform Rejection-Free from that step. For each step of PNS within the local maximum area of three states, the Markov Chain has the probability of 25% to include neither of the remaining neighbors from the three states. Thus, PNS helped the Markov chain to escape from this local maximum area. In addition, in the middle part of the PNS chain, when the target density value of the PNS chain is increasing, we usually have more than one important neighbor. For example, if we have three important neighbors, we only have 12.5% for considering none by PNS.

Thus, the PNS is better than Rejection-Free because the PNS performs much better than the Rejection-Free algorithm when the local maximum areas trap the Markov chain. On the other hand, PNS performs similar to Rejection-Free when the Markov chain is increasing with respect to the target density value.

This section uses 50% random partial neighbors for each step. We have many other choices, and we will consider and compare these choices in the next section.

6 Optimal subset choice for Partial Neighbor Search

Before we start our Markov chain, we have a proposal distribution \mathcal{Q} with a corresponding neighbor set \mathcal{N} where $\mathcal{N}(x) := \{y \in \mathcal{S} \mid \mathcal{Q}(x, y) > 0\}$. A Partial Neighbor Set means any function \mathcal{N}_i satisfies the following conditions:

1. $\mathcal{N}_i : \mathcal{S} \rightarrow \mathbb{P}(\mathcal{S})$, where \mathcal{S} is the state space, and $\mathbb{P}(\mathcal{S})$ is the power set of \mathcal{S} ;
2. $\mathcal{N}_i(x) \subset \mathcal{N}(x), \forall x \in \mathcal{S}$;
3. $y \in \mathcal{N}_i(x) \iff x \in \mathcal{N}_i(y), \forall x, y \in \mathcal{S}$;

Usually, we want to pick \mathcal{N}_i such that $|\mathcal{N}_i(x)| < |\mathcal{N}(x)|$ to perform proper PNS. In addition, to ensure irreducibility, we need to make sure $\cup_{k=1}^K \mathcal{N}_k(x) = \mathcal{N}(x)$ for all $x \in \mathcal{S}$. The corresponding proposal distribution is defined to be $\mathcal{Q}_i(x, y) : \mathcal{S} \times \mathcal{S} \rightarrow \mathbb{R}$, where $\mathcal{Q}_i(x, y) \propto \mathcal{Q}(x, y)$ for $y \in \mathcal{N}_i(x)$ and $\mathcal{Q}_i(x, y) = 0$ otherwise.

Here, we compare the four different ways to choose the proposal distribution $\{\mathcal{Q}_k, \mathcal{N}_k\}$ for PNS in the (\star) step in Algorithm 5 by the 200×200 QUBO question we discussed in Sect. 4:

- Method A (random subset every step): The Partial Neighbor Sets \mathcal{N}_k are randomized for every step, where $|\mathcal{N}_k(x)| = \frac{1}{2} \times |\mathcal{N}(x)| = 100$. \mathcal{Q}_k 's are defined accordingly.
- Method B (random subset every ten steps): The Partial Neighbor Sets \mathcal{N}_k are randomized for once ten steps, where $|\mathcal{N}_k(x)| = \frac{1}{2} \times |\mathcal{N}(x)| = 100$. That is, $\mathcal{N}_{10 \times k + 1} = \mathcal{N}_{10 \times k + 2} = \dots = \mathcal{N}_{10 \times k + 10}$ for $\forall k \in \mathbb{N}$. \mathcal{Q}_k 's are defined accordingly.
- Method C (systematic subset every step): Before we start our Markov Chain, we define two Partial Neighbor Sets \mathcal{N}_1 and \mathcal{N}_2 , where $|\mathcal{N}_1(x)| = |\mathcal{N}_2(x)| = \frac{1}{2} \times |\mathcal{N}(x)| = 100, \mathcal{N}_1(x) \cap \mathcal{N}_2(x) = \emptyset$. For step k of the Markov chain, we only randomly generate $r_k \in \{1, 2\}$, and apply \mathcal{N}_{r_k} for step k . \mathcal{Q}_1 and \mathcal{Q}_2 are defined accordingly.
- Method D (systematic subset every ten steps): Before we start our Markov Chain, we define two Partial Neighbor Sets \mathcal{N}_1 and \mathcal{N}_2 , where $|\mathcal{N}_1(x)| = |\mathcal{N}_2(x)| = \frac{1}{2} \times |\mathcal{N}(x)| = 100, \mathcal{N}_1(x) \cap \mathcal{N}_2(x) = \emptyset$. For every ten steps of the Markov chain, we only randomly generate $r_k \in \{1, 2\}$ and apply \mathcal{N}_{r_k} . That is $r_{10 \times k + 1} = r_{10 \times k + 2} = \dots = r_{10 \times k + 10}$ for $\forall k \in \mathbb{N}$. \mathcal{Q}_1 and \mathcal{Q}_2 are defined accordingly.

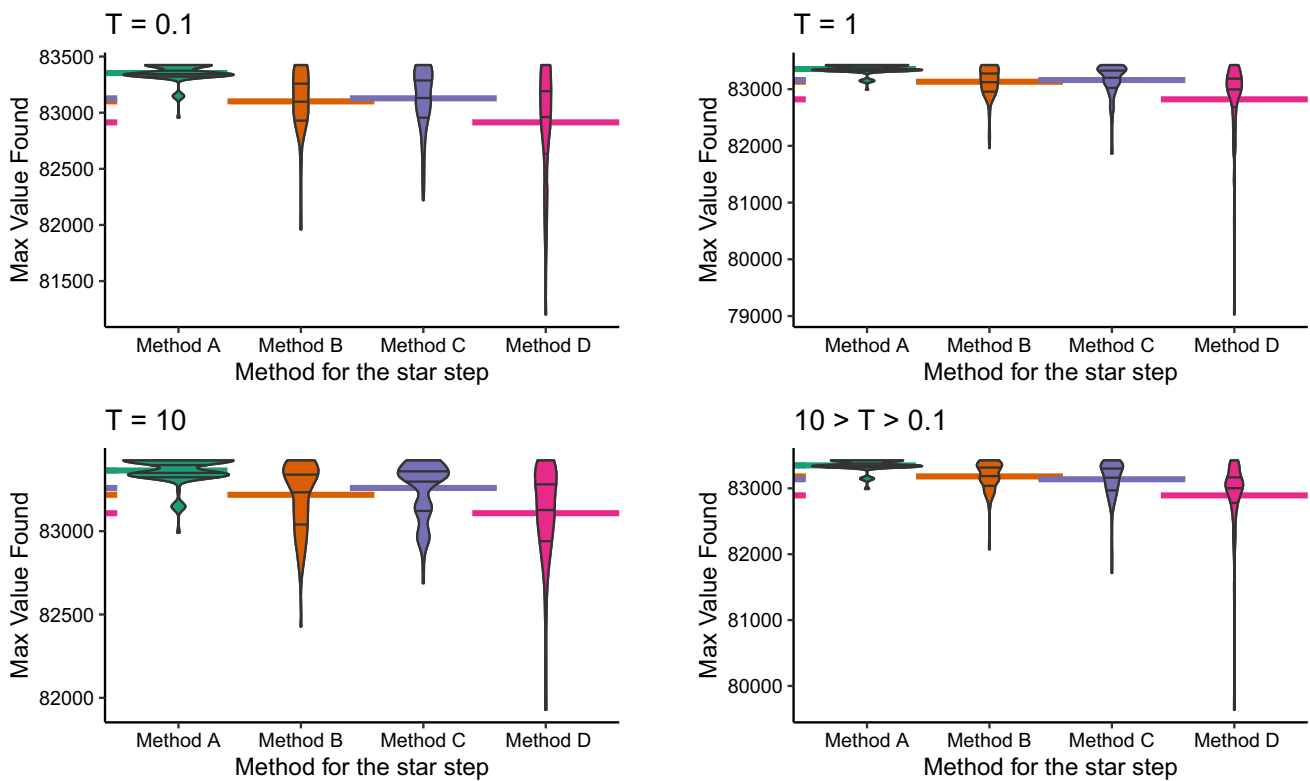


Fig. 4 Comparison of different methods to choose the subsets for PNS, in terms of the highest (log) target density value $\log \pi(x) = x^T Qx$ found. Method A: random subset every step; method B: random subset every ten steps; method C: systematic subset every step; method D: systematic subset every ten steps. Random upper triangular QUBO matrix where the non-zero elements are generated by $Q_{i,j} \sim N(0, 100^2)$. Four

different cooling schedules where $T = 0.1, 1,$ and 10 for all n , and T being geometric from 10 to 0.1 , are used here. The number of iterations for all methods is 1000 . The three black lines inside the violin plots are $25\%, 50\%$, and 75% quantile lines. The colored segments represent the mean values. (Color figure online)

For this 200×200 QUBO example, the settings for the simulation are the same as in Sect. 4. For Method C and D, the two Partial Neighbor Sets \mathcal{N}_1 and \mathcal{N}_2 are defined as flipping the first 100 entries in x and flipping the last 100 entries in x . The result for the simulation is shown in Fig. 4. This figure shows that the random subset at every step (Method A) performs the best in all four Cooling Schedules. Therefore, we will keep using Method A in all later parts.

In addition, we used Partial Neighbor Sets with half elements from all neighbors in previous simulations. Now we compare the Partial Neighbor Sets with cardinality of $|\mathcal{N}(x)| \times \{1, \frac{3}{4}, \frac{2}{3}, \frac{1}{2}, \frac{1}{3}, \frac{1}{4}, \frac{1}{5}, \frac{1}{6}, \frac{1}{7}, \frac{1}{8}\}$ by the same simulation settings as before. From Fig. 5, we can see that $\frac{1}{3}, \frac{1}{4}, \frac{1}{5}$ are overall the best among all the choices. Thus, we can conclude that Partial Neighbor Sets with around 25% of the neighbors being considered at each step are the best for the above QUBO question.

Therefore, we conclude that our best method to do optimization for the 200×200 QUBO question is Algorithm 6.

Algorithm 6 Partial Neighbor Search for the 200 by 200 QUBO question

```

initialize  $J_0$ 
for  $k$  in 1 to  $K$  do
  randomly pick  $\mathcal{N}_k(J_{k-1}) \subset \mathcal{N}(J_{k-1})$  where  $|\mathcal{N}_k(J_{k-1})| = 50$ 
  ▷ Only 50 out of the 200 neighbors will be considered
  for  $Y \in \mathcal{N}_k(J_{k-1})$  do
    calculate  $q(Y) = \min\{1, [\frac{\exp(Y^T Q Y)}{\exp(J_{k-1}^T Q J_{k-1})}]^{\frac{1}{T(k)}}\}$ 
    ▷ the transition prob. from  $J_{k-1}$  to  $Y$ 
  end for
  choose  $J_k \in \mathcal{N}_k(J_{k-1})$  such that  $\hat{P}(J_k = Y | J_{k-1}) \propto q(Y)$ 
  ▷ choose the next Jump Chain State
end for
    
```

7 Comparison with Tabu Rejection-Free algorithm

Tabu search (Glover 1989, 1990) is also a methodology in optimization that guides a local heuristic search procedure to

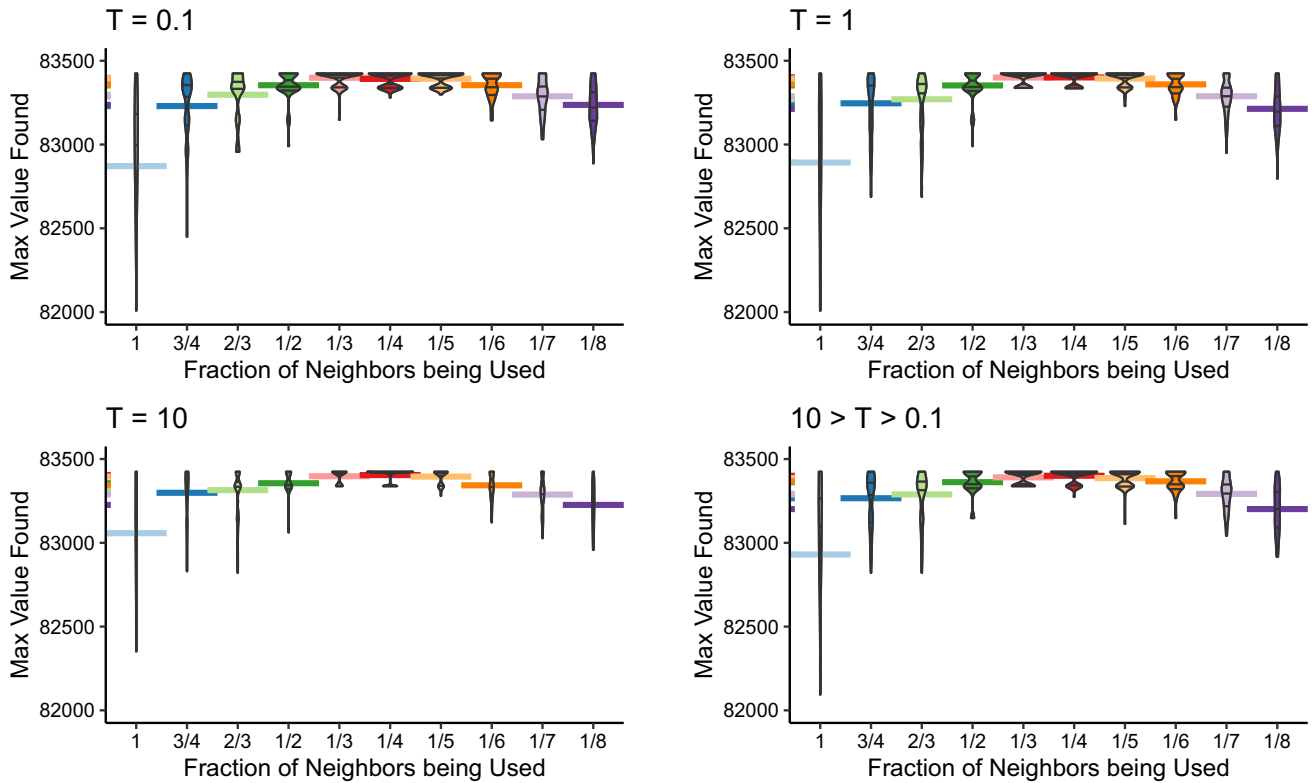


Fig. 5 Comparison of different sizes of the random subsets for PNS, in terms of the highest (log) target density value $\log \pi(x) = x^T Qx$ being found. Subset sizes are $N \times \{1, \frac{3}{4}, \frac{2}{3}, \frac{1}{2}, \frac{1}{3}, \frac{1}{4}, \frac{1}{5}, \frac{1}{6}, \frac{1}{7}, \frac{1}{8}\}$. Random upper triangular QUBO matrix where the non-zero elements are generated by $Q_{i,j} \sim N(0, 100^2)$. Four different cooling schedules

where $T = 0.1, 1, \text{ and } 10$ for all n , and T being geometric from 10 to 0.1, are used here. The number of iterations for all methods is 1000. The three black lines inside the violin plots are 25%, 50%, and 75% quantile lines. The colored segments represent the mean values. (Color figure online)

explore the solution space beyond local optimality. The idea of Tabu search is to prohibit access to specific previously-visited solutions. Tabu search is the most intuitive method to help the Markov Chain escape from local maximum areas, as in Fig. 1. After moving from state A to state B, we must choose our next state among $\{B_1, B_2, \dots, B_N\}$. We can combine our Rejection-Free algorithm for optimization with Tabu search and then compare this new method to the PNS by the QUBO question. Note that we do not need to record all visited states since we are almost impossible to revisit a state after a certain number of steps. Thus, we only need to record the last several steps and prohibit our Markov chain from revisiting them. The new algorithm is formulated as Algorithm 7.

We compare PNS with L -step Simplified Tabu Rejection-Free for $L = 1, 2, 3, \dots, 9$. Again, we randomly generate a 200 by 200 upper triangular QUBO matrix. The non-zero elements from the 200 by 200 upper triangular matrix Q were generated randomly with $Q_{i,j} \sim N(0, 100^2)$ for $i < j$. Note that we need to consider about 200 neighbors at each step for Rejection-Free and Simplified Tabu Rejection-Free, while we only need to consider 50 neighbors at each iteration for PNS. If we proceed with the algorithms

Algorithm 7 L steps Simplified Tabu Rejection-Free for optimization

```

initialize  $J_0$ 
for  $k$  in 1 to  $K$  do
  for  $Y \in \mathcal{N}(J_{k-1}) \setminus \{J_{k-2}, \dots, J_{k-L-1}\}$  do
    ▷ Remove states from the last  $L$  steps
     $q(Y) = \min\{1, [\frac{\exp(Y^T Q Y)}{\exp(J_k^T Q J_k)}]^{\frac{1}{T(k)}}\}$ 
    ▷ the transition prob. from  $J_{k-1}$  to  $Y$ 
  end for
  choose  $J_k \in \mathcal{N}_k(J_{k-1})$  such that  $\hat{P}(J_k = Y | J_{k-1}) \propto q(Y)$ 
  ▷ choose the next Jump Chain State
end for
    
```

with a single-core implementation, Rejection-Free and Tabu Rejection-Free need about four times longer than PNS with the same number of steps. Therefore, we can compare the PNS with $4 \times 100 = 400$ iterations with the other methods to get a fair comparison for the program on a single core. Note that we are using this many steps here because 400 steps are enough for PNS to find a good enough answer. The result for the simulation is shown in Fig. 6. From this plot, we can see that PNS performs much better than Rejection-Free and Simplified Tabu Rejection-Free.

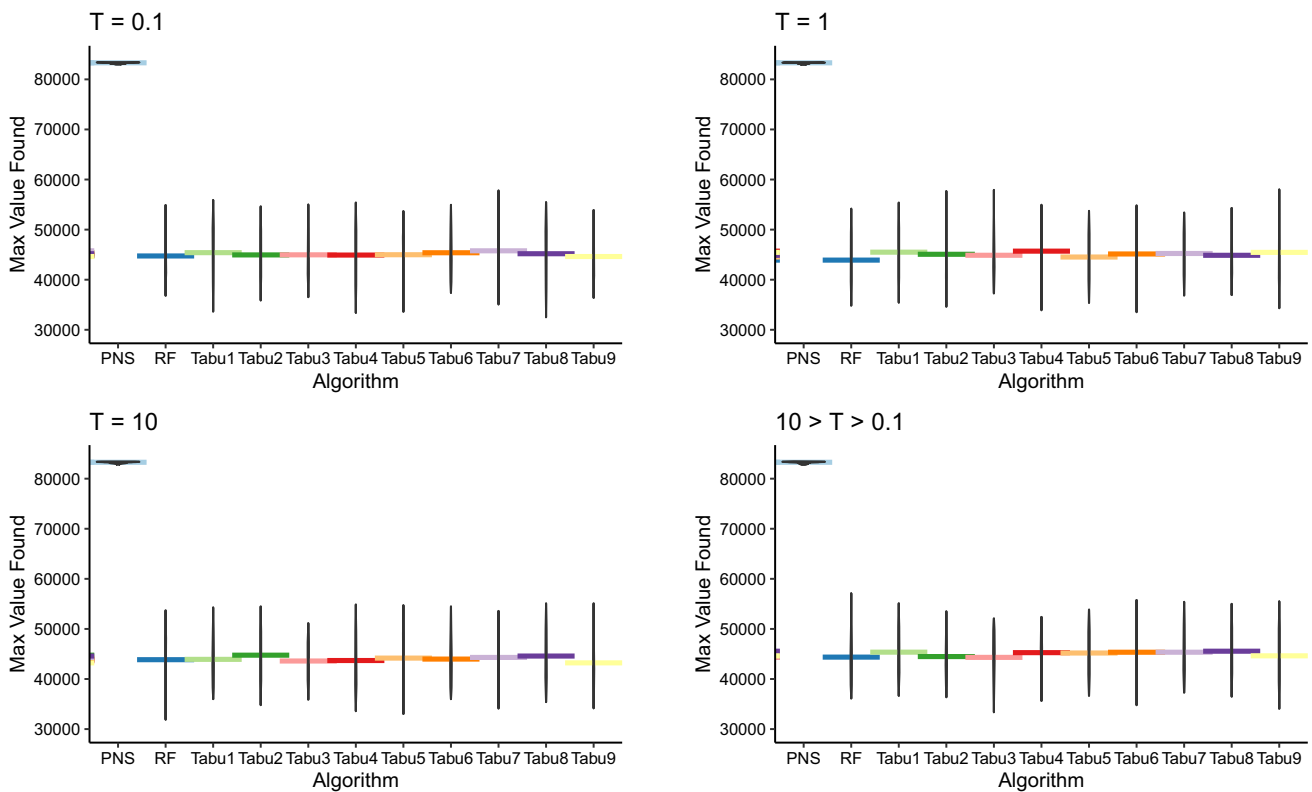


Fig. 6 Comparison of PNS, Rejection-Free, and 1-Step to 9-steps Simplified Tabu Rejection-Free, in terms of the highest (log) target density value $\log \pi(x) = x^T Qx$ found. Random upper triangular QUBO matrix where the non-zero elements are generated by $Q_{i,j} \sim N(0, 100^2)$. Four different cooling schedules where $T = 0.1, 1, \text{ and } 10$ constantly, and T

being geometric from 10 to 0.1, are used here. The run time for all algorithms on a single-core implementation is about the same. The number of iterations for PNS is 400, and the number of iterations for all other methods is 100. The colored segments represent the mean values. (Color figure online)

8 Application to Knapsack problem

The Knapsack problem is another well-known NP-hard problem in optimization (Salkin and De Kluyver 1975). We consider the simplest 0-1 Knapsack problem here. Given a knapsack of max capacity W and N items with corresponding values $\{v_i\}_{i=1}^N$ and weights $\{w_i\}_{i=1}^N$, we want to find a finite number of items among all N items which can maximize the total value while not exceeding the max capacity of the knapsack. That is, for given $W > 0, \{v_i\}_{i=1}^N > 0$ and $\{w_i\}_{i=1}^N > 0$, find a sequence of N binary variable $\{x_i\}_{i=1}^N \in \{0, 1\}$ to maximize

$$\sum_{i=1}^N v_i x_i$$

subject to $\sum_{i=1}^N w_i x_i \leq W$ (7)

Since the Knapsack problem is NP-hard, we can use the Simulated Annealing algorithm to find a feasible solution. For this simulation, we set $W = 100,000$. We randomly

generate $N = 1000$ items where the values and weights are random by $w_i, v_i \sim \text{Poisson}(1000)$. The mean and the variance for $\text{Poisson}(1000)$ are both 1000. Suppose we want to find a binary vector $x = (x_1, x_2, \dots, x_N)^T$ of dimension N to maximize $v^T x$ subject to $w^T x \leq W$.

Again, we used a uniform proposal distribution among all neighbors where the neighbors are defined as binary vectors with Hamming distance 1. That is, $Q(x, y) = \frac{1}{N}$ for $\forall y \in \mathcal{N}(x)$, where $y \in \mathcal{N}(x) \iff |x - y| = \sum_{i=1}^N |x_i - y_i| = 1, \forall x, y \in \{0, 1\}^N$. We randomly choose half of the neighbors at each step for PNS. That is, $|\mathcal{N}_k(x)| = \frac{1}{2}|\mathcal{N}(x)| = 500$ for $\forall x \in \{0, 1\}^N$. Moreover, the target density $\pi(x) = \mathbb{1}(w^T x \leq W) \times v^T x$, where $\mathbb{1}$ represents the indicator function. In addition, $T(k)$ represents the temperature at step k for the Cooling Schedule here.

Again, we compare Simulated Annealing, Rejection-Free, and PNS here. The result is shown in Fig. 7. The plot shows that Rejection-Free for optimization and PNS algorithm are better than the regular Simulated Annealing algorithm in all four Cooling Schedules. Again, for the simulation shown in Fig. 7, the numbers of iterations used for the three methods are set to be different to have a fair comparison between the

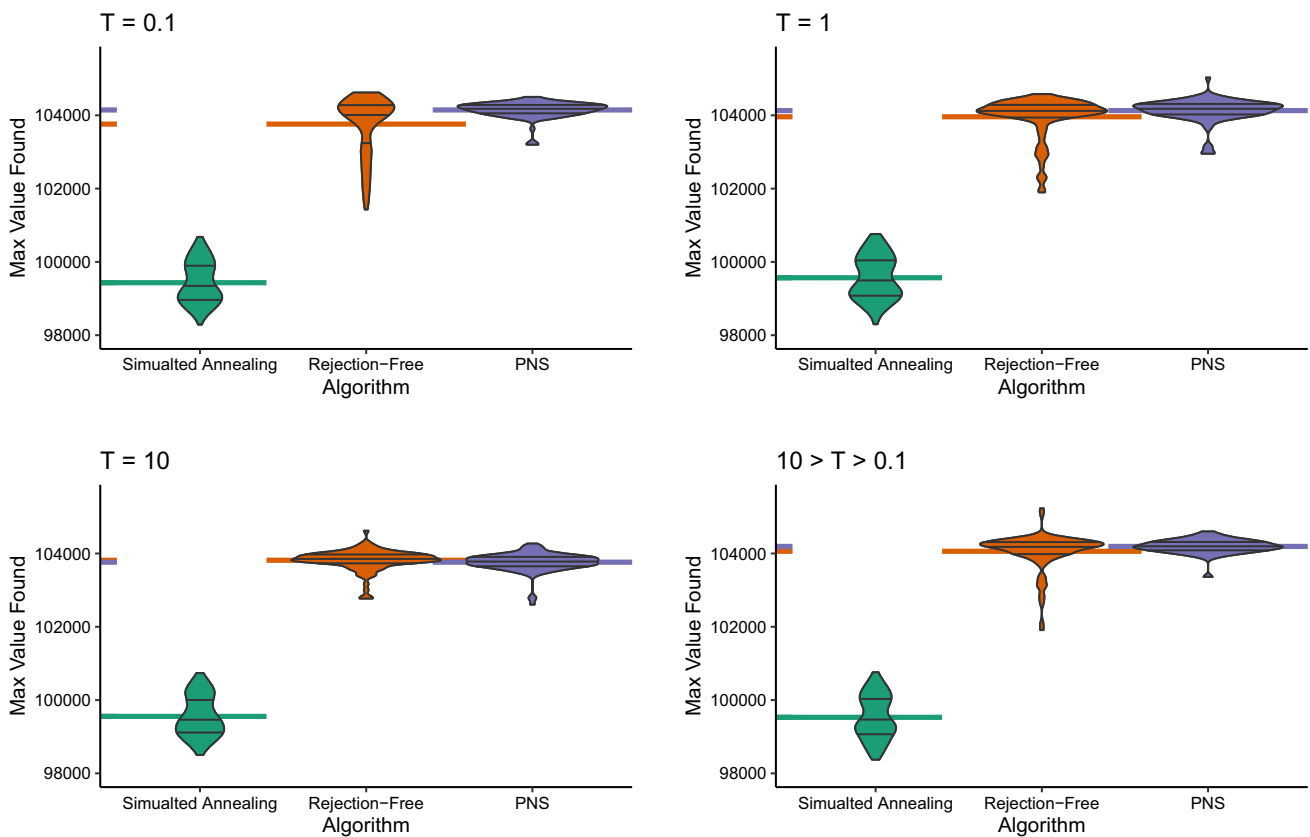


Fig. 7 Comparison of Simulated Annealing, Rejection-Free, and PNS in terms of the highest target density values found in Knapsack Problem with $W = 100,000, N = 1000, w_i, v_i \sim \text{Poisson}(1000)$. Four different cooling schedules where $T = 0.1, 1, \text{ and } 10$ constantly, and T being geometric from 10 to 0.1, are used there. The number of iterations for

Simulated Annealing is 1,000,000, while the number for Rejection-Free and PNS is 1000. The three black lines inside the violin plots are 25%, 50%, and 75% quantile lines. The colored segments represent the mean values. (Color figure online)

three methods. We set the number of iterations for Simulated Annealing to be 1000,000. The numbers of iterations for Rejection-Free and PNS are 1000 since we need to consider 1000 neighbors at each iteration for Rejection-Free for optimization. In contrast, we only need to consider one neighbor for each iteration in Simulated Annealing.

This result shows that PNS is not always that much better than Rejection-Free when the number of iterations is the same. In some cases, where the target density is not sharply peaked, and there are few local extreme areas, Rejection-Free can also perform excellently. Note that if we run the above simulation on a single core, PNS will only take about half of the time used by Rejection-Free, and if we use parallel hardware to apply the above algorithm, Rejection-Free, and PNS will take about the same time.

In addition, Rejection-Free is not always better than simple Simulated Annealing. For example, there will be no rejections if $\pi(x) \equiv 1$ for all $x \in \mathcal{S}$. The Simulated Annealing will move to a new state by computing a single probability, while the Rejection-Free will do the same but

compute the probabilities for all neighbors. However, when the dimension of the problem is large, or the target density is sharply peaked, the PNS will perform much better than Rejection-Free, and Rejection-Free will perform much better than Simulated Annealing.

9 Application to 3R3XOR problem

The 3R3XOR problem is a methodology for generating benchmark problem sets for Ising machines devices designed to solve discrete optimization problems cast as Ising models introduced by Hen (2019). The Ising model, named after Ernst Ising, is concerned with the physics of magnetic-driven phase transitions (Cipra 1987). The Ising model is defined on a lattice, where a spin $s_i \in \{-1, 1\}$ is located on each lattice site (Block and Preis 2012). The optimization question for the Ising model has been widely applied to many scientific problems such as neuroscience (Hopfield 1982) and environmental science (Ma et al. 2014). Thus, algorithms, even

special-purpose programmable devices, designed to solve discrete optimization problems cast as Ising models are popular (Hen 2019), and our PNS algorithm is one of them.

However, the non-planar Ising model is NP-complete (Cipra 2000). We cannot find an optimal state from an Ising model in polynomial time. Then, it is hard for us to compare the performance of the heuristic solvers, such as Rejection and PNS, by the time used to find the optimal state from a random Ising model. On the other hand, Hen (2019) introduced a tool for benchmarking Ising machines in 2019. In his approach, linear systems of equations are cast as Ising cost functions. The linear systems can be solved quickly, while the corresponding Ising model exhibits the features of NP-hardness (Hen 2019). This way, we can construct special Ising models with a unique known optimal state. Then we can use these special Ising models to compare the heuristic solvers' runtimes to find the optimal state.

This section focuses on constructing a simplified version of 3-body Ising with N spins from a binary linear system of N equations. The simplified version is defined as follows:

$$H(\{s_j\}) = \sum_{a < b < c} \mathbf{M}_{a,b,c} s_a s_b s_c, \tag{8}$$

where $s_i \in \{-1, 1\}$ for $\forall i = 1, 2, \dots, N$. $\mathbf{M}_{a,b,c}$ is a $N \times N \times N$ matrix where $\mathbf{M}_{a,b,c} = 0 \forall a \geq b, b \geq c, \text{ or } a \geq c$.

In Hen's (2019) approach, we start by choosing a binary matrix $\{\mathbf{A}_{i,j}\}$ and a binary vector $\{\mathbf{b}_j\}$ to form a modulo two linear system of N equations in N variables.

$$\sum_{j=1}^N \mathbf{A}_{i,j} x_j \equiv \mathbf{b}_i \pmod 2, \text{ for } i = 1, 2, \dots, N. \tag{9}$$

This modulo two linear system of equations can always be solved in polynomial time using Gaussian elimination. In addition, as long as the binary matrix $\{\mathbf{A}_{i,j}\}$ is invertible, the solution, if it exists, is unique. Suppose $\{x_1, \dots, x_n\}$ are n binary variables. Then for given $\{\mathbf{A}_{i,j}\}$ and $\{\mathbf{b}_j\}$, we define

$$F(\{x_j\}) = \sum_{i=1}^N \mathbb{1} \left(\sum_{j=1}^N \mathbf{A}_{i,j} x_j \not\equiv \mathbf{b}_i \pmod 2 \right), \tag{10}$$

where $\mathbb{1}$ means indicator function here. Since F is a sum of N indicator functions, then $0 \leq F \leq N$ and the minimum bound is reached when $\{x_j\}$ is the solution to the modulo two linear system.

Let $s_j = 1 - 2x_j \in \{-1, 1\}$ for $j = 1, 2, \dots, N$ be N Ising spins. Then we must have

$$\prod_{j:\mathbf{A}_{i,j}=1} s_j = (-1)^{\mathbf{b}_i} \text{ if and only if } \sum_{j=1}^N \mathbf{A}_{i,j} x_j \equiv \mathbf{b}_i \pmod 2, \tag{11}$$

$\forall i = 1, 2, \dots, m$. Then

$$\begin{aligned} F &= \sum_{i=1}^N \mathbb{1} \left(\sum_{j=1}^N \mathbf{A}_{i,j} x_j \not\equiv \mathbf{b}_i \pmod 2 \right) \\ &= \sum_{i=1}^N \mathbb{1} \left(\prod_{j:\mathbf{A}_{i,j}=1} s_j \not\equiv (-1)^{\mathbf{b}_i} \right), \\ &\text{since } \prod_{j:\mathbf{A}_{i,j}=1} s_j \text{ and } (-1)^{\mathbf{b}_i} \in \{-1, 1\} \\ &= \frac{1}{2} \left[\sum_{i=1}^N \left(1 - (-1)^{\mathbf{b}_i} \prod_{j:\mathbf{A}_{i,j}=1} s_j \right) \right]. \end{aligned} \tag{12}$$

After dropping immaterial constants, we define

$$F_0(\{s_j\}) = \sum_{i=1}^N \left[(-1)^{\mathbf{b}_i} \prod_{j:\mathbf{A}_{i,j}=1} s_j \right]. \tag{13}$$

Note that $F \geq 0$ and the minimum bound is reached when $\{x_j\}$ is the solution to the modulo two linear system. Thus, $F_0 \leq N$, and the maximum bound will be reached when $\{x_j \mid x_j = \frac{1}{2}(1 - s_j)\}$ is the solution to the modulo 2 linear system. In addition, as long as the matrix $\{\mathbf{A}_{i,j}\}$ is invertible, the solution to the equation system must uniquely exist, and then there must exist a single configuration maximizes F_0 whose maximum value is exactly N .

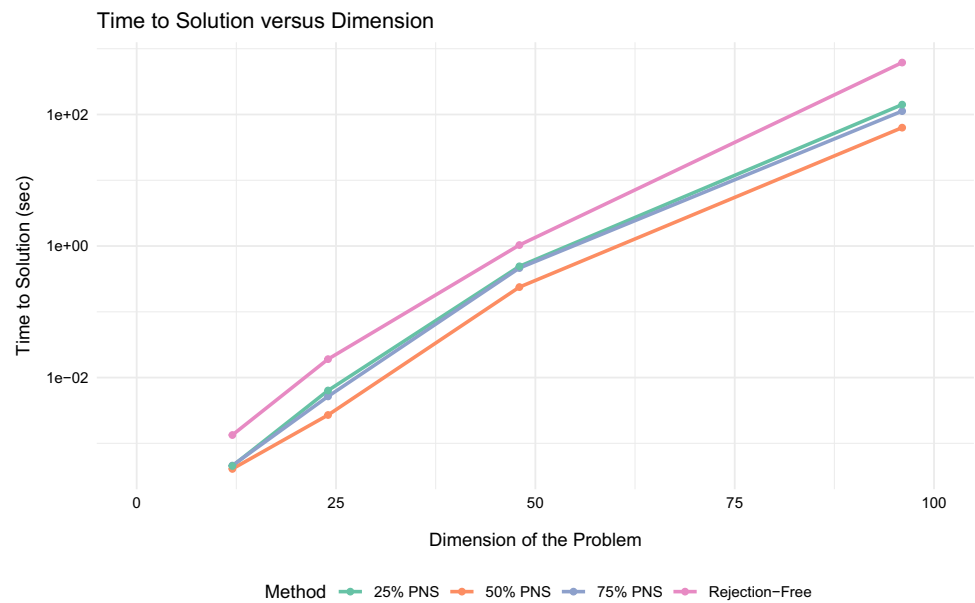
Again, the Hamiltonian for simplified 3-body Ising model including only the cubic term to be $H(\{s_j\}) = \sum_{a < b < c} \mathbf{M}_{a,b,c} s_a s_b s_c$. Here, we assume, on each row of the binary matrix $\{\mathbf{A}_{i,j}\}$, $\sum_{j=1}^N \mathbf{A}_{i,j} = 3$. Then, let $\mathbf{M}_{a,b,c} = (-1)^{\mathbf{b}_i}$ if $\exists i, a < b < c$ such that $\mathbf{A}_{i,a} = \mathbf{A}_{i,b} = \mathbf{A}_{i,c} = 1$, and $\mathbf{M}_{a,b,c} = 0$ otherwise. Then, we have $H(\{s_j\}) = F_0(\{s_j\})$.

Thus, we can construct an Ising model with a unique optimal bound with a known optimal value N as follows:

1. find an invertible binary matrix $\{\mathbf{A}_{i,j}\}$ and a binary vector $\{\mathbf{b}_i\}$, where $\sum_{j=1}^N \mathbf{A}_{i,j} = 3, \forall i$
2. solve the modulo 2 linear equation system $\sum_{j=1}^N \mathbf{A}_{i,j} x_j \equiv \mathbf{b}_i \pmod 2$, for $i = 1, 2, \dots, N$ to make sure the unique solution exists
3. define $\mathbf{M}_{a,b,c}$ be a $N \times N \times N$ matrix where $\mathbf{M}_{a,b,c} = (-1)^{\mathbf{b}_i}$ if $\exists i, a < b < c$ such that $\mathbf{A}_{i,a} = \mathbf{A}_{i,b} = \mathbf{A}_{i,c} = 1$, and $\mathbf{M}_{a,b,c} = 0$ otherwise
4. then we must have a unique optimal solution s_{\max} for $H(s_{\max}) = \max(H(s)) = N$

By constructing the special 3-body $N \times N \times N$ Ising model with a unique optimal solution of maximum bound N , we can examine the performance of the Rejection-Free and PNS algorithms on these special Ising models. Again,

Fig. 8 Comparison of the minimum value for the time used to find the optimal state by Rejection-Free and PNS with 25%, 50%, and 75% of the neighbors being considered at each step for a random Ising model generated by 3R3XOR. Each dot represents the median of 50 repeated simulations for a given problem size $N = 12, 24, 48, \text{ and } 96$



uniform proposal distributions are used here, and the neighbors are defined as binary vectors with Hamming distance 1. We randomly generate the special Ising models with four different sizes $N = 12, 24, 48, \text{ and } 96$. For each of these four different sizes, we generate 50 different Ising models and record the time used by the algorithms to reach their individual optimal states. The median of these 50 results for both Rejection-Free and PNS algorithms are shown in Fig. 8. From this figure, Rejection-Free is the worst. 25% PNS performs comparably to 75%, and the 50% PNS performs the best.

10 Application to Continuous State Space

In previous sections, we focused on optimization questions with the discrete state space S where all states have, at most, a finite number of neighbors. Meanwhile, Simulated Annealing also works for general state space, where the number of neighbors can be uncountable. In addition, Theorem 13 in Rosenthal et al. (2021) extended the Rejection-Free sampling to general state space. Similarly, we can extend the Rejection-Free optimization to general state space.

Although we have a solid theory base for Rejection-Free sampling in general state space (Rosenthal et al. 2021), applying Rejection-Free sampling to those cases is challenging. A significant difficulty is involved in the for loop that calculates the transition probability of all neighbors in Algorithm 4. In continuous cases, although numerical integration of all transition probability can be performed, such tasks are unlikely to be efficiently divided among specialized hardware with a certain number of parallel processing units. A similar challenge holds for Rejection-Free optimization as well. On the

other hand, PNS, as described in Algorithm 5, can be applied straightforwardly to continuous cases by choosing the Partial Neighbors Sets $\mathcal{N}_k(x)$ to be finite subsets of all the neighbors $\mathcal{N}(x)$ in Algorithm 5.

We compare the performance of Simulated Annealing with our PNS on a simple example of quadratic programming, which belongs to the category of continuous optimization, as stated below:

$$\begin{aligned}
 & \arg \max x^T Qx \\
 & \text{subject to } x_i \geq 0, \forall i = 1, 2, \dots, N \\
 & \sum_{i=1}^N x_i = 1,
 \end{aligned} \tag{14}$$

where Q is a given an upper triangular N by N matrix and $x \in \mathbb{R}^N$. For most cases, the quadratic programming is stated by $\arg \min$ instead of $\arg \max$. We use the $\arg \max$ version here to be consistent with the QUBO question in Sect. 4, and $\arg \max$ is equivalent to $\arg \min$ when replacing Q by $-Q$. This quadratic programming question is also NP-hard as long as Q is indefinite (Sahni 1974), where indefinite means matrices that are neither positive semi-definite nor negative semi-definite.

We randomly generate a 200 by 200 upper triangular to be the matrix Q , where the non-zero elements from the 200 by 200 upper triangular matrix Q were generated randomly by $Q_{i,j} \sim \text{Normal}(0, 100^2), \forall i \leq j$. We compare Simulated Annealing and PNS in 100 simulation runs here. We omit Rejection-Free since applying Rejection-Free to continuous cases is quite challenging.

The target density value is set to be $\pi(x) = \exp\{x^T Qx\}$, $\forall x$ such that $x_i \in (0, 1), \forall i = 1, 2, \dots, N$, and $\pi(x) = -\infty$

otherwise. In addition, the proposal distribution \mathcal{Q} and the corresponding neighbor set \mathcal{N} are defined as follows:

1. for state $x = (x_1, x_2, \dots, x_N)^T \in \mathcal{S}$, choose a random entry x_r for $r \in \{1, 2, \dots, N\}$;
2. generate a random value $s \sim \text{Normal}(0, 0.1^2)$;
3. let $y_r = x_r + s$ and $y_n = x_n \times \frac{1-x_r}{1-y_r}, \forall n \neq r$;
4. if $y_r \notin (0, 1)$, then the corresponding $\pi(y)$ is defined to be $-\infty$; in practice, we just need to generate a new y ; also note that, as long as $y_r, x \in (0, 1)$, we must have $y \in (0, 1)^N$;
5. to ensure the reversibility within each Partial Neighbor Set, we also consider $y'_r = x_r - s$ and $y'_n = x_n \times \frac{1-x_r}{1-y'_r}, \forall n \neq r$; if $y'_r \notin (0, 1)$, then we can ignore y' .

With the given steps, we have $\sum_{n=1}^N y_n = 1$ as long as $\sum_{n=1}^N x_n = 1$. This method is similar to component-wise Simulated Annealing. We find a random component, magnify or minify it, and then modify the rest of the entries to keep the summation unchanged. This proposal distribution \mathcal{Q} is therefore systematic. By the above ways to generate neighbors, we can eliminate the constraints that $x_i \geq 0, \forall i = 1, 2, \dots, N$, and $\sum_{i=1}^N x_i = 1$, and we only need to focus on arg max $x^T Qx$.

In addition, some papers such as Bierkens (2016), Neal (2004) claim that the non-reversible MCMC is more efficient than the reversible MCMC. For the previous discrete examples, their proposal distributions are intuitively reversible since we always consider states with flipped bits as neighbors. Thus, we test the efficiency of non-reversible MCMC here with our continuous example. To get a non-reversible PNS, Step 5 from the method to choose the reversible partial neighbor set there shall be ignored to get the non-reversible PNS, and we just need to do Steps 1 to 4.

For Simulated Annealing, we randomly generate one neighbor by the above-given steps and calculate the transition probability. For both reversible and non-reversible PNS, we can generate, for example, 20 random neighbors in total at each step. In this case, the reversible Partial Neighbor Set \mathcal{N}_i is only a random subset with \mathcal{N} with 20 elements, which are 10 pairs of states created by reversibility, and the non-reversible Partial Neighbor Set is simply 20 random states from the proposal distribution. The implementation of both versions of PNS is simple compared to the Rejection-Free since Rejection-Free needs to consider uncountable many neighbors.

The result for the simulation is shown in Fig. 9. We can see that both reversible and non-reversible PNS performs better than Simulated Annealing in all four different cooling schedules. However, the difference between PNS and Simulated Annealing in this continuous example is not as much as the difference between the algorithms from the discrete QUBO

questions. Note that the continuous example is not as sharply peaked as the discrete example from Sect. 6. Thus, after we choose a random entry r , we only need to move a small step around the original value of x_r . On the other hand, we have to flip between 0 and 1 in the discrete example. Thus, the rejection rate for the Simulated Annealing is lower than the rate from the discrete example, so the performance of these algorithms gets closer than the discrete cases. In addition, the non-reversible PNS does not outperform the reversible PNS, which means the non-reversible PNS does not always solve the optimization questions more efficiently. However, the results may differ for other examples, which can be one of our future research directions.

In addition, PNS is specially designed for parallelism hardware. Again, with a specialized dedicated processor such as DAU, PNS can yield 100x to 10,000x speedups (Sheikholeslami 2021). In addition, this example also shows that PNS has more flexibility compared to the Rejection-Free algorithm. Again, Rejection-Free can hardly work for cases with infinite neighbors, while PNS can be easily applied by choosing finite \mathcal{N}_k .

Moreover, the number of elements in \mathcal{N}_k needs to be reasonable for PNS to keep its performance. For example, if we used $|\mathcal{N}_k| = 500$, we would calculate too many transition probabilities at each step, making the algorithm inefficient. Meanwhile, if we used $|\mathcal{N}_k| = 2$, the number of Partial Neighbor Sets being considered at each step would be too few. As PNS will force the Markov chain to move to one element from the Partial Neighbor Set \mathcal{N}_k , it will move to some terrible choices of states when all states in the Partial Neighbor Set \mathcal{N}_k have small target density values. In the above simulation, choosing $|\mathcal{N}_k|$ from 10 to 30 is the best strategy, and the numbers between 10 and 30 perform similarly.

Furthermore, especially for the continuous cases, using a new partial neighbor set at each step is the key for PNS to get good performance. If we keep using the same partial neighbors for too many steps, the Markov chain may be forced to go somewhere wired, and thus, the efficiency of such PNS won't be that good.

11 Summary

In this paper, we have demonstrated new methods for optimization questions based on the Markov chain Monte Carlo. Rejection-Free can improve the optimization efficiency over Simulation Annealing by considering all the neighbors simultaneously. Also, PNS optimization was introduced to address the problem that local maximum areas may trap the Markov chains. PNS works better than Rejection-Free and Simulated Annealing in the four optimization examples illustrated in this paper. Three sets of discrete examples have been simulated to demonstrate that PNS can produce signif-

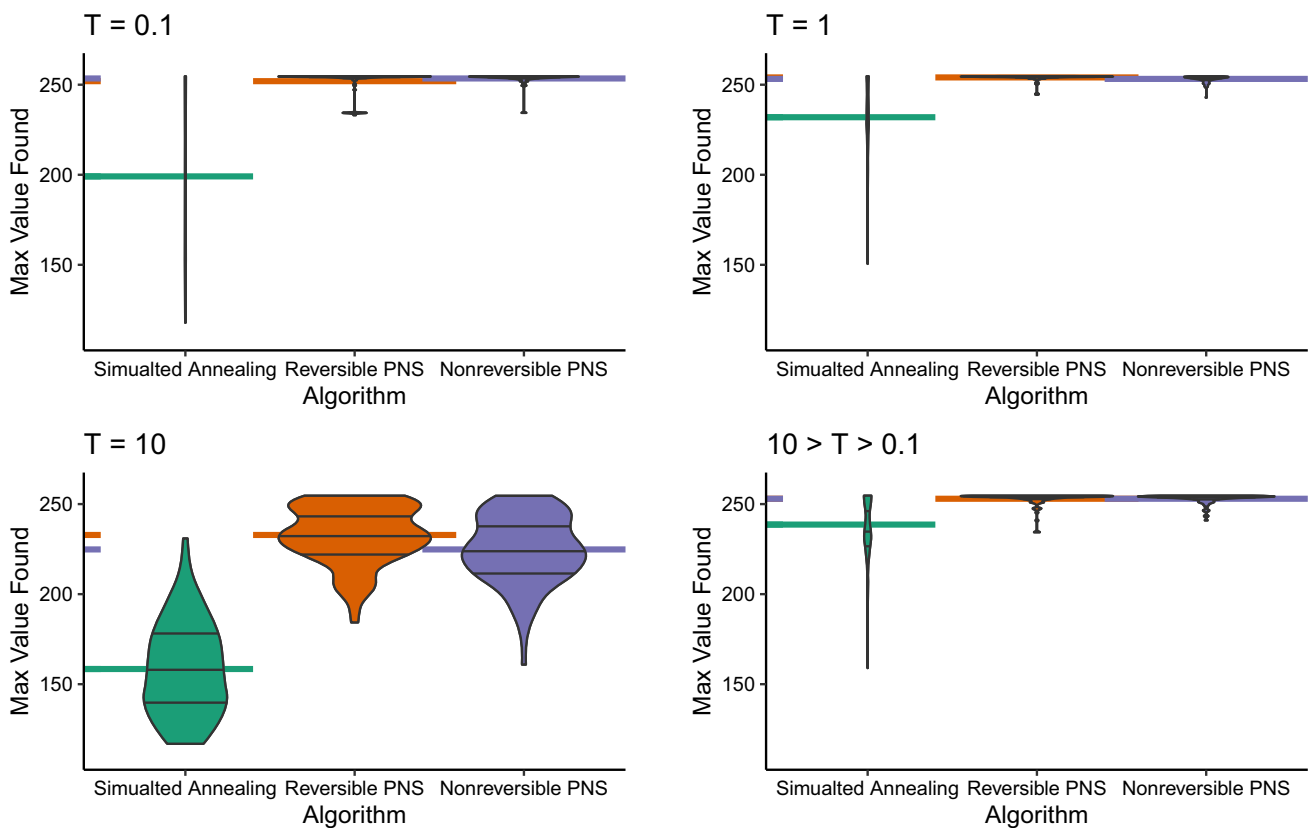


Fig. 9 Comparison of Simulated Annealing and PNS in terms of the highest (log) target density value $\log \pi(x) = x^T Q x$ being found, for a random upper triangular matrix Q and $x \in \mathbb{R}^N$ subject to $x_i \geq 0$, $\forall i = 1, 2, \dots, N$, and $\sum_{i=1}^N x_i = 1$. The non-zero elements are generated by $Q_{i,j} \sim N(0, 100^2)$. Four different cooling schedules where $T(k) = 0.1, 1$, and 10 constantly, and $T(k)$ being geometric from 10

to 0.1 are used here. The number of iterations for Simulated Annealing is $200,000$, and the number of iterations for both reversible and non-reversible PNS is $24,000$. The run times for these three algorithms on a single-core implementation are around 30 s. The three black lines inside the violin plots are 25% , 50% , and 75% quantile lines. The colored segments represent the mean values. (Color figure online)

icant speedups in optimization problems. PNS has also been applied to one continuous example to demonstrate its greater flexibility than Rejection-Free.

Besides the Rejection-Free sampling paper (Rosenthal et al. 2021), we have also applied PNS to the sampling cases (Chen et al. 2022). We have proven the convergence theorem for the PNS sampling algorithm. Under some specific conditions, the Markov chain produced by PNS sampling will converge to the target density almost surely. On the other hand, PNS optimization illustrated by this paper does not need such strict conditions for convergence. For the three conditions described in Sect. 6, the third condition $y \in \mathcal{N}_i(x) \iff x \in \mathcal{N}_i(y)$ related to the reversibility of the Markov chain can be somehow loosened. A fascinating question is how much we can loosen the conditions. For example, non-reversible PNS can be useful in optimization questions. We tried one non-reversible PNS in Sect. 10, and the result shows that the non-reversible PNS is just as good as the reversible PNS. We believe that non-reversible PNS

can be helpful under other circumstances, and it can be one of our future research directions.

The limitation of PNS is that if we apply it on parallelism hardware, especially for chips not specially designed for parallel computing, the speed will be slower than desired. This algorithm needs different processors to communicate frequently. For example, on my personal computer, using sixteen processors to do PNS can only reduce 50% of the time required by the program compared to one processor. On the other hand, if we use specialized hardware such as DAU (Matsubara et al. 2020), the time used for communication between processors will be much shorter.

Acknowledgements The authors thank Fujitsu Ltd. and Fujitsu Consulting (Canada) Inc. for providing financial support. The authors thank the reviewers and editors for very careful readings and helpful comments which have greatly improved the manuscript.

Author Contributions SC and JSR designed the algorithm, did most of the simulation, and wrote the main manuscript text. Aki Dote proposed the idea of Partial Neighbor Search at the very beginning and provided advice during the process. Hirotaka Tamura did the simulation in section

9 and provided advice during the process. AS coordinated everything for the team and provided advice during the process. All authors reviewed the manuscript.

Declarations

Conflict of interest The authors declare no competing interests.

References

- Albright, B.: An introduction to simulated annealing. *Coll. Math. J.* **38**(1), 37–42 (2007)
- Beichl, I., Sullivan, F.: The Metropolis algorithm. *Comput. Sci. Eng.* **2**(1), 65–69 (2000)
- Bertsimas, D., Tsitsiklis, J.: Simulated annealing. *Stat. Sci.* **8**(1), 10–15 (1993)
- Bianchi, L., Dorigo, M., Gambardella, L.M., et al.: A survey on metaheuristics for stochastic combinatorial optimization. *Nat. Comput.* **8**(2), 239–287 (2009)
- Bierkens, J.: Non-reversible metropolis-hastings. *Stat. Comput.* **26**(6), 1213–1228 (2016)
- Block, B., Preis, T.: Computer simulations of the Ising model on graphics processing units. *Eur. Phys. J. Spec. Top.* **210**(1), 133–145 (2012)
- Chen, S., Rosenthal, J.S., Dote, A., et al.: Sampling via rejection-free partial neighbor search (2022). arXiv preprint [arXiv:2210.10513](https://arxiv.org/abs/2210.10513)
- Cipra, B.A.: An introduction to the Ising model. *Am. Math. Mon.* **94**(10), 937–959 (1987)
- Cipra, B.A.: The Ising model is NP-complete. *SIAM News* **33**(6), 1–3 (2000)
- Douc, R., Robert, C.P.: A vanilla Rao-Blackwellization of Metropolis-Hastings algorithms. *Ann. Stat.* **39**(1), 261–277 (2011)
- Floudas, C.A., Pardalos, P.M.: *Encyclopedia of Optimization*, pp. 1538–1542. Springer, Berlin (2008)
- Garey, M.R., Johnson, D.S., Stockmeyer, L.: Some simplified NP-complete problems. In: *Proceedings of the Sixth Annual ACM Symposium on Theory of Computing*, pp. 47–63 (1974)
- Glover, F.: Tabu search-part I. *ORSA J. Comput.* **1**(3), 190–206 (1989)
- Glover, F.: Tabu search-part II. *ORSA J. Comput.* **2**(1), 4–32 (1990)
- Glover, F., Kochenberger, G., Du, Y.: A tutorial on formulating and using QUBO models (2018). [arXiv:1811.11538](https://arxiv.org/abs/1811.11538)
- Hen, I.: Equation planting: a tool for benchmarking Ising machines. *Phys. Rev. Appl.* **12**(011), 003 (2019)
- Hintze, J.L., Nelson, R.D.: Violin plots: a box plot-density trace synergism. *Am. Stat.* **52**(2), 181–184 (1998)
- Hitchcock, D.B.: A history of the Metropolis-Hastings algorithm. *Am. Stat.* **57**(4), 254–257 (2003)
- Hopfield, J.J.: Neural networks and physical systems with emergent collective computational abilities. *Proc. Natl. Acad. Sci.* **79**(8), 2554–2558 (1982)
- Kirkpatrick, S., Gelatt, C.D., Vecchi, M.P.: Optimization by simulated annealing. *Science* **220**(4598), 671–680 (1983)
- Kochenberger, G., Hao, J.K., Glover, F., et al.: The unconstrained binary quadratic programming problem: a survey. *J. Comb. Optim.* **28**(1), 58–81 (2014)
- Ma, Y.P., Sudakov, I., Strong, C., et al.: Ising model for melt ponds on Arctic sea ice. (2014). [arXiv:1408.2487](https://arxiv.org/abs/1408.2487)
- Matsubara, S., Takatsu, M., Miyazawa, T., et al.: Digital annealer for high-speed solving of combinatorial optimization problems and its applications. In: *2020 25th Asia and South Pacific Design Automation Conference (ASP-DAC)*, pp. 667–672 (2020)
- Metropolis, N., Rosenbluth, A.W., Rosenbluth, M.N., et al.: Equation of state calculations by fast computing machines. *J. Chem. Phys.* **21**(6), 1087–1092 (1953)
- Neal, R.M.: Improving asymptotic variance of MCMC estimators: non-reversible chains are better. arXiv preprint [arXiv:math/0407281](https://arxiv.org/abs/math/0407281) (2004)
- Nikolaev, A.G., Jacobson, S.H.: Simulated annealing. *Handbook of metaheuristics*, pp. 1–39 (2010)
- Rosenthal, J.S., Dote, A., Dabiri, K., et al.: Jump Markov chains and rejection-free Metropolis algorithms. *Comput. Stat.* **36**(4), 2789–2811 (2021)
- Rutenbar, R.A.: Simulated annealing algorithms: an overview. *IEEE Circuits Devices Mag.* **5**(1), 19–26 (1989)
- Sahni, S.: Computationally related problems. *SIAM J. Comput.* **3**(4), 262–279 (1974)
- Salkin, H.M., De Kluyver, C.A.: The knapsack problem: a survey. *Naval Res. Logist. Q.* **22**(1), 127–144 (1975)
- Schrijver, A.: On the history of combinatorial optimization (till 1960). *Handb. Oper. Res. Manag. Sci.* **12**, 1–68 (2005)
- Sheikholeslami, A.: The power of parallelism in stochastic search for global optimum: Keynote paper. In: *ESSCIRC 2021—IEEE 47th European Solid State Circuits Conference (ESSCIRC)*, pp. 36–42 (2021)
- Sodan, A.C., Machina, J., Deshmeh, A., et al.: Parallelism via multi-threaded and multicore CPUs. *Computer* **43**(3), 24–32 (2010)

Publisher's Note Springer Nature remains neutral with regard to jurisdictional claims in published maps and institutional affiliations.

Springer Nature or its licensor (e.g. a society or other partner) holds exclusive rights to this article under a publishing agreement with the author(s) or other rightsholder(s); author self-archiving of the accepted manuscript version of this article is solely governed by the terms of such publishing agreement and applicable law.